The TRANSP-0 framework for integrated transportation and power system design

Dominik Ascher
Fakultät für Informatik
Technische Universität München
85748 Garching bei München, Germany
Email: ascher@in.tum.de

Georg Hackenberg
Fakultät für Informatik
Technische Universität München
85748 Garching bei München, Germany
Email: hackenbe@in.tum.de

***Abstract*— Increasing penetration of decentralized energy production as well as the propagation of new transportation paradigms such as transportation electrification, autonomous vehicles and mobility-on-demand will require interrelated key changes to current transportation and power systems. To diminish negative environmental impacts and achieve longterm sustainability, close integration between transportation and power systems is necessary and integrated planning, operation and control strategies have to be established. In this paper, we present TRANSP-0, a system design framework for rapid formulation and evaluation of design options within integrated transportation and power systems. Firstly, we present the TRANSP-0 design space in terms of the static parameters for integrated subsystem design. Secondly, we visit the dynamic properties of subsystem design by formulating the underlying optimal control problem. Thirdly, we establish the requirements to integrated control strategies in terms of objectives and constraints of the described optimal control problem. Finally, we conclude with an outlook on the future scope of the proposed system design framework.**

I. MOTIVATION AND DIFFERENTIATION

High numbers of electric vehicles (EV) and renewable energy sources (RES) will require fundamental changes to current transportation and power systems. For the power system, uncontrolled charging of a high number of EVs can impose increased peak loads within the distribution network [1], while increasing levels of fluctuating RES loads will impose challenges to power system operation [2]. However, previous research has shown the ability of plug-in electric vehicles (PEVs) to contribute to balancing the load fluctuations of intermittent RES [3]. Allan et al. [4] consider a crucial challenge for successful EV adaption to consist in their integration with supporting infrastructure, i.e. the transportation system, the electric power grid and supporting information systems constituting the intelligent transportation system (ITS).

To comprehensively address the demands of integrated transportation and power systems, integrated planning, operation and control strategies have to be established. According strategies are frequently addressed within the concept of *vehicle-to-grid (V2G)* [5], which enables scheduling for charging or discharging EV batteries during times of increased power availability or demand within the power system. Widespread V2G adoption provides mutual benefits for transport and energy sectors [6], possesses the potential to significantly reduce the amount of excess energy produced within the power system [7], and facilitates both environmental and economic benefits [8], [9]. More specifically, key benefits of V2G include reduction of emissions as well as increased efficiency, stability and reliability of the power system [10].

In the context of V2G, methods for intelligent *scheduling* of EV charging/discharging are widely discussed as key approaches to integrate EVs into the power grid [11]. To sufficiently address technical and economic objectives, Andreotti et al. [12] argue for better suitability of multi-objective optimization methods over single-objective optimization methods for plug-in vehicles operation in terms of model effectiveness. To achieve optimal charging decisions, Ota et al. [13] propose a decentralized V2G control scheme addressing the intermittency of RES energy production using electric vehicles. In contrast, approaches for *vehicle routing* describe optimizing route selection for traffic participants and focus on control strategies for route selection/driving. Felipe et al. [14] propose multiple heuristics for routing EVs, which consider different partial recharge strategies and technologies while traveling along routes. Towards integrating both scheduling and routing approaches, Barco et al. [15] present an approach for minimizing operation cost for battery EV fleets, which achieves optimal routing and charge scheduling performance. Then, in the field of *modeling and simulation*, Galus et al. [16] combine power system models, agent based transport simulations and modeling to investigate the impact of electric mobility on integrated transportation and power systems. Finally, Junaibi et al. [17] assess the technical feasibility of EV penetration within integrated systems by microscopically modeling traffic and power flows and ITS.

Problems: While the presented scheduling methods heavily address control strategies for EVs within the power system, they neglect their effects on the transportation system. In contrast, routing approaches heavily address control strategies for optimally routing single or multiple EVs within the transportation system, but do not incorporate a more detailed representation of the power system and it's underlying objectives. Finally, approaches within the field of modeling and simulation have targeted integrated transportation and power system modeling and simulation in the past. However, employed control strategies are based

on a fixed set of objectives and constraints and focus on assessing EV impact. However, the importance of integrated planning for integrating electric and transportation sectors has been shown in the past [18]. In summary, we found that current approaches do not sufficiently support planning and control of integrated transportation and power systems, i.e. the formulation and evaluation of future transportation and power system design options and alternatives.

Contributions: To address this situation, in this paper we extend our previous work [19], [20], [21] and present a formal system design framework for rapid and iterative formulation and evaluation of design options within integrated transportation and power systems. For this we describe the underlying design space in terms of static parameters for integrated subsystem design in Section II. Then, we describe the dynamic properties of subsystem design by formulating the underlying optimal control problem in Section III. Finally, we establish the requirements to integrated control strategies in terms of objectives and constraints of the described optimal control problem in Section IV.

II. The TransP-0 design space

The TransP-0 design framework is intended to support both transportation and power system engineers during early project phases in formulating and evaluating different design options quickly. Therefore, transportation and energy system properties - both static and dynamic - have to be captured sufficiently precise. On the other hand, the design abstraction should omit unnecessary details to enable frequent design iterations. With these requirements in mind we have developed a candidate design abstraction, which comprises various transportation and energy subsystem parameters. Note that we focused on using a minimum number of parameters, considering potentially decreased physical accuracy. However, to capture the real-world environment precisely and establish a well-founded terminology, it is important to establish formal definitions.

Subsequently we formally describe the design space parameters for the transportation subsystem in Section II-A and the energy subsystem in Section II-B.

A. Transportation subsystem

We decided to model the transportation subsystem in a mesoscopic fashion [22]. In particular, our model includes a representation of the road network and the individual vehicles. The road network is modeled as a directed graph, where nodes represent intersections and edges represent road segments. Hereby, the edge weight defines the number of lanes and the edge direction indicates the intended driving direction. Vehicles are assigned to points on the edges of the road network. Hence, vehicles are able to move along edges and switch between edges at intersections. The TransP-0 abstraction of the transportation subsystem is illustrated in Figure 1.

Formally, the transportation subsystem TS of the integrated design abstraction is modeled as a tuple (TI, TP), where

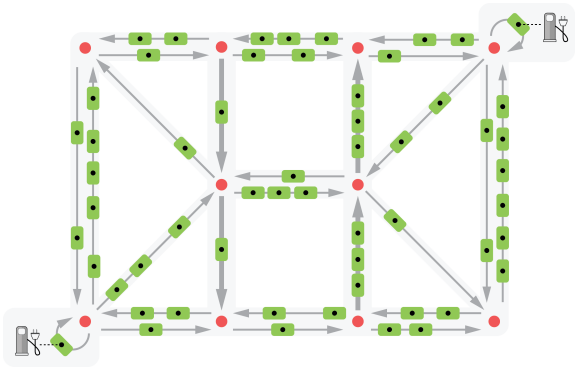

Fig. 1. Representation of the transportation subsystem including an infrastructure (i.e. *red* road intersections and *gray* segments) and *green* participants.

- TI represents the *transportation infrastructure* and
- TP represents the *traffic participants*.

Essentially, we distinguish between the static (i.e. the infrastructure) and the dynamic (i.e. the participants) parts of the transportation subsystem. In the following, we describe the the infrastructure design abstraction in Section II-A.1 before explaining the participant design abstraction in Section II-A.2.

1) Infrastructure: The transportation infrastructure TI is modeled as a tuple (RI, RS), where

- RI represents the *road intersections* and
- RS represents the *road segments*.

Road intersections describe the nodes of the directed graph, while road segments describe the edges instead. Subsequently, we first describe road intersections in Section II-A.1.a before explaining road segments in Section II-A.1.b.

a) Intersections: The road intersections RI are modeled as a tuple (RIL, RIC), where

- RIL represents a finite set of road intersection *labels* and
- $RIC : RIL \to \mathbb{R}^3$ represents their geometric *coordinates*.

b) Segments: Instead, the road segments RS are modeled as a five-tuple $(RSL, RSS, RST, RSC, RSE)$, where

- RSL represents a finite set of road segment *labels*,
- $RSS/RST : RSL \to RIL$ represent their respective *source* and *target* road intersection labels while accounting for possible self-edges,
- $RSC : RSL \to \mathbb{N}$ represents their *capacities* (i.e. the number of lanes of the road segment), and
- $RSE : RSL \to \mathbb{R}^+$ represents their *efficiency* (i.e. a friction coefficient of the road segment).

Note that the previous parameters completely determine our road segment model. Consequently, we abstract from a variety of parameters typically considered in microscopic models such as continuous elevation profiles. However, our model supports arbitrary discretization as distance between intersections and the length of edges can be chosen arbitrarily.

Furthermore, we derive the road segment distance $RSD : RSL \to \mathbb{R}_0^+$ as a mapping from road segment labels to distances using the Euclidean metric $E : \mathbb{R}^3 \times \mathbb{R}^3 \to \mathbb{R}_0^+$ such that

$$RSD(rsl) = E(RIC(RSS(rsl)), RIC(RST(rsl))).$$

Finally, we define road segment positions $RSP \subseteq RSL \times \mathbb{R}_0^+$ as tuples of road segment labels and traveled distances

$$RSP = \{(rsl, d) \in RSL \times \mathbb{R}_0^+ \mid d \leq RSD(rsl)\}.$$

We use the road segment positions RSP to locate traffic participants (i.e. vehicles) on the transportation infrastructure as explained in the following section.

2) Participants: The traffic participants TP are modeled as a tuple (V, D), where

- V represents the *vehicles* and
- D represents the *demands*.

Consequently, we - again - distinguish between static (i.e. the vehicles) and dynamic (i.e. the demands) properties of the model. In the following, we first describe the vehicle design abstraction in Section II-A.2.a before explaining the demand design abstraction in Section II-A.2.b.

a) Vehicles: The vehicles V are modeled as a seven-tuple $(VL, VSE, VME, VP_0, VC, VEE, VSOC_0)$, where

- VL represents a finite set of vehicle *labels*,
- $VSE : VL \to \mathbb{R}^+$ represents their *sizes* (i.e. the length of the vehicle in road segment direction),
- $VME : VL \to \mathbb{R}^+$ represents their *mechanical efficiencies* (i.e. the conversion coefficient between employed energy and driven distance similar to [23]),
- $VP_0 : VL \to RSP$ represents their initial road segment *positions* (see Section II-A.1.b),
- $VC : VL \to \mathbb{R}^+$ represents their battery *capacities* (i.e. the maximum amount of energy that can be stored by the vehicle),
- $VEE : VL \to \mathbb{R}^+$ represents their *electrical efficiencies* (i.e. the conversion coefficient between employed and stored energy),
- $VSOC_0 : VL \to \mathbb{R}^+$ represents their initial *state of charges* (i.e. the amount of energy stored by the vehicle initially) such that

$$\forall vl \in VL : VSOC_0(vl) \leq VC(vl).$$

Note that we again abstract from many parameters which can be considered in microscopic models [23] such as vehicle weight or exact vehicle geometry. In particular, we approximate mechanical and electrical efficiencies with constants only.

b) Demands: Finally, the demands D are modeled as a four-tuple (DL, DV, DP, DT), where

- DL represents a finite set of demand *labels*,
- $DV : DL \to VL$ represents the demands *vehicle* labels (i.e. the concerned vehicle),
- $DP : DL \to RSP$ represents the demands road segment *positions* (i.e. where the concerned vehicle is expected to be), and
- $DT : DL \to \mathbb{N}^+$ represents the demands *time* points (i.e. when the concerned vehicle is expected to be there).

Note that our abstraction is based on discrete time (see Section III). However, we do not prescribe the time step resolution. For long travel distances and durations more coarse resolutions can be used, while for shorter distances and durations more fine-grained resolutions are typically needed.

B. Power / energy subsystem

Similar to the transportation subsystem (see Section II-A), we decided to model the energy subsystem in a mesoscopic fashion [19]. Note that microscopic models represent the individual power lines and their physical characteristics [24], while macroscopic models aggregate the entire energy subsystem into a single marketplace without power line characteristics [25]. Our mesoscopic model takes an intermediate approach, where only selected characteristics of the network topology are represented. In particular, we limit our representation to subnetworks of equal voltage level (i.e. the network *regions*) and their hierarchical connectivity through transformers. Consequently, balances can be computed also for single regions rather than the entire electricity market. The TRANSP-0 abstraction of the energy subsystem is illustrated in Figure 2.

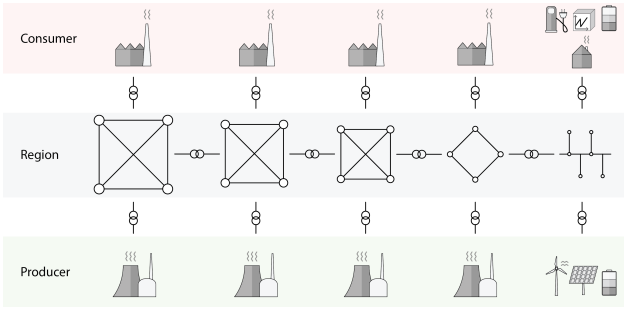

Fig. 2. Illustration of an energy subsystem design including an infrastructure (i.e. regions) and components (i.e. producers and consumers).

Formally, the energy subsystem ES of the integrated design abstraction is modeled as a tuple (EI, EC), where

- EI represents the *energy infrastructure* and
- EC represents *energy components*.

Hence, we separate network characteristics and network usage. Subsequently, we first explain the infrastructure in Section II-B.1.a before describing the components in Section II-B.2.

1) Infrastructure: The energy infrastructure EI is modeled as a one-tuple (R), where

- R represents the *regions* of the energy infrastructure, which are determined by the voltage levels and transformers of the network.

Note that we selected a region model [19] over a power flow model [24] to reduce modeling effort and increase computational efficiency. Hence, we think it is important to enable rapid formulation and evaluation. In the following, we describe the regions in Section II-B.1.a.

a) Regions: The network regions R are modeled as a four-tuple (RL, RC, RE, RP), where

- RL represents a finite set of region labels,
- $RC : RL \to \mathbb{R}^+$ represents their *capacities* (i.e. the maximum amount of energy that can flow through each region in a predefined time interval),
- $RE : RL \to \mathbb{R}^+$ represents their *efficiencies* (i.e. a constant factor determining the energy that is lost while flowing through that region), and
- $RP : RL \to RP \cup \{\bot\}$ represents their *parent* regions (i.e. the superordinate voltage level or the start symbol $\bot$ for the root level).

Note that our region model represents the energy system as a tree structure. The nodes of the tree represent *subnetworks* with distinct voltage levels. The edges of the tree represent *transformers* connecting the subnetworks instead. The region model can be derived from existing network topologies easily.

2) Components: Instead, the energy components EC are modeled as a three-tuple (SL, ES, CS), where

- SL represents the *static loads*,
- ES represents the *energy storages*, and
- CS represents the *charging stations*.

In the following, we first explain the static load design abstraction in Section II-B.2.a, before describing the energy storage design abstraction in Section II-B.2.b and presenting the charging station design abstraction in Section II-B.2.c. Note that currently we do not include energy producers such as generators as well as smart consumers. However, these components are subject for our future work.

a) Static loads: The static loads SL are modeled as a three-tuple (SLL, SLP, SLR), where

- SLL represents a finite set of static load *labels*,
- $SLP : SLL \to (\mathbb{N} \to \mathbb{R})$ represents their static load *profiles* (i.e. a predefined production and consumption curve), and
- $SLR : SLL \to RL$ represents their parent *regions* (i.e. the region where the static load is attached).

Note that static load profiles associate a numeric load to each discrete time step. Hereby positive loads represent energy production and negative loads represent energy consumption. Consequently, static loads can be used to model everything from home appliances over solar panels to conventional power generators. In particular, we assume such loads to be uncontrollable from the perspective of the engineers.

b) Energy storages: Then, the energy storages ES are modeled as a five-tuple $(ESL, ESC, ESE, ESS_0, ESR)$, where

- ESL represent a finite set of energy storage *labels*,
- $ESC : ESL \to \mathbb{R}^+$ represents their *capacities* (i.e. the maximum amount of energy that can be stored),
- $ESE : ESL \to \mathbb{R}^+$ represents their energy storage *efficiencies* (i.e. the conversion coefficient between and stored energy), and
- $ESS_0 : ESL \to \mathbb{R}_0^+$ represents their initial *state of charges* (i.e. the amount of energy stored initially) such that

$$ESS_0(esl) \leq ESC(esl), \text{ and}$$

- $ESR : ESL \to RL$ represents their parent *regions* (i.e. the region where the energy storage is attached).

Note that the energy storage model is analogous to the electric vehicle model described in Section II-A.2.a. However, electric vehicles additionally define mechanical parameters, while energy storages are attached to regions statically. Furthermore, we currently target small batteries rather than large storage facilities. Note that the latter might require additional parameters.

c) Charging stations: Finally, the charging stations CS are modeled as a four-tuple (CSL, CSE, CSP, CSR), where

- CSL represents a finite set of charging station *labels*,
- $CSE : CSL \to \mathbb{R}^+$ represents their *efficiencies* (i.e. a constant loss factor for respective energy flows), and
- $CSP : CSL \to RSL$ represents their *positions*, i.e. road segment labels with zero road segment distance

$$RSD(CSP(csl)) = 0, \text{ and}$$

- $CSR : CSL \to RL$ represents their parent *regions* (i.e. the region where the charging station is attached).

Note that the charging station position mapping CSP and the charging station region mapping CSR define the static connections between the transportation subsystem and the energy subsystem. Consequently, vehicles (see Section II-A.2.a) are able to interact with arbitrary regions (see Section II-B.1.a) of the energy subsystem infrastructure at predefined zero-length road segments (see Section II-A.1.b).

III. Discrete-time TransP-0 dynamics

While the previous section was only concerned with the static parameters, i.e. the design space of integrated transportation and energy system design, this section focuses on dynamic aspects instead. In effect, each system design defines an optimal control problem (or dynamic programming problem) [26] over the transportation and energy subsystem dynamics. We decided to use a discrete-time model of the system dynamics due to the high problem dimensionality involved in its control. In the following, we describe the respective state space in Section III-A, the action space in Section III-B, and the transition function in Section III-C. Note that the states, actions, and transition function do not have to be defined by the transportation and power system engineers. Rather, the definitions are equal for all system designs expressed with the TransP-0 abstraction.

A. States

The overall system states $S_t \in \mathbb{S}$ with time point $t \in \mathbb{N}$ of the optimal control problem are modeled as a four-tuple $(VS_t, ESS_t, CSS_t, RS_t)$, where

- VS_t represents the *vehicle states*,
- ESS_t represents the *energy storage states*,
- CSS_t represents the *charging station states*, and
- RS_t represents the *region states*.

Note that we do not associate a state with the infrastructure of the transportation subsystem (i.e. we assume the infrastructure to be constant). In the following, we describe the vehicle states in Section III-A.1, the energy storage states in Section III-A.2, the charging station station states in Section III-A.3, and the region states in Section III-A.4.

1) Vehicle states: The vehicle states VS_t are modeled as a tuple $(VP_t, VSOC_t)$, where

- $VP_t : VL \rightarrow RSP$ represents their current road segment *positions* and
- $VSOC_t : VL \rightarrow \mathbb{R}_0^+$ represents their current *state of charge*.

Consequently, our design abstraction neglects effects such as changing vehicle weights due to passenger load or changing tire and road friction coefficients [27]. Instead, we omitted such effects to ease design formulation [23] and employed mechanical efficiency coefficients VME (see Section II-A.2.a), which have to be selected carefully to achieve desired effects.

2) Energy storage states: In contrast, the energy storage states ESS_t are modeled as a one-tuple $(ESOC_t)$, where

- $ESOC_t : ESL \rightarrow \mathbb{R}_0^+$ represents their current *state of charge*.

Note that we omitted advanced effects such as wear of equipment, which can cause degrading storage efficiency. Again, we believe that such effects can be neglected during early phase system-level design. Furthermore, depending on the time step resolution additional state parameters are required to model - for example - ramp-up times of pumped storage hydro power plants [28].

3) Charging station states: Then, the charging stations states CSS_t are modeled as a one-tuple (CSB_t), where

- $CSB_t : CSL \rightarrow \mathbb{R}$ represents their current *balance* (i.e. the energy transferred from or to a connected vehicle).

In an advanced version of the design abstraction one could also consider failure states or software control states of charging stations. For now we assume that all charging stations work properly. Furthermore, the control strategy is provided implicitly by the optimal control problem formulation.

4) Region states: Finally, the region states R_t are modeled as a three-tuple $(RE_t^<, RE_t^>, RB_t)$, where

- $RE_t^\sim : RL \rightarrow \mathbb{R}, \sim \in \{<, >\}$ represents their current aggregate *energy* production (i.e. $\sim =>$) and consumption (i.e. $\sim =<$) values (obtained from the subregions and subcomponents) and
- $RB_t : RL \rightarrow \mathbb{R}$ represents their current *balances* (i.e. the aggregated loads).

Again, we neglect physical state parameters such as power line temperatures or failure modes (e.g. due to exceeded temperature limits or due to environmental influences). Consequently, we assume that the energy subsystem infrastructure is available during entire system operation. In an advanced version of the design abstraction one might also consider failure modes and respective repair actions [29] as well as additional topological and physical characteristics.

B. Actions

The actions $A_t \in \mathbb{A}$ with time point $t \in \mathbb{N}$ of the optimal control problem are modeled as a tuple (VA_t, ESA_t), where

- VA_t represents the *vehicle actions* and
- ESA_t represents the *energy storage actions*.

Note that vehicles and energy storages are the only system components comprising actions. The states of the other components is influenced directly or indirectly by these actions. In the following, we describe the vehicle actions in Section III-B.1 before explaining the energy storage actions in Section III-B.2.

1) Vehicle actions: The vehicle actions VA_t are modeled as a three-tuple (VR_t, VS_t, VB_t), where

- $VR_t : VL \rightarrow (\mathbb{N} \rightarrow RSL)$ represents their respective *route*, i.e. a sequence of connected road segments with $\forall vl \in VL, n \in \mathbb{N}$:

$$RST(VR_t(vl)(n)) = RSS(VR_t(vl)(n+1))$$

  starting at the previous vehicle road segment position with $\forall vl \in VL$ and $VP_{t-1}(vl) = (rsl, d)$:

$$VR_t(vl)(0) = rsl,$$

- $VS_t : VL \rightarrow \mathbb{R}_0^+$ represents their current *speed*, and
- $VB_t : VL \rightarrow \mathbb{R}$ represents their current *balances* (i.e. the amount of energy transferred from or to a charging station) such that

$$\forall vl \in VL : VB_t(vl) \neq 0 \text{ only if}$$

  the current vehicle speed is zero, i.e.

$$VS_t(vl) = 0 \text{ and}$$

  the vehicle is located currently at a charging station, i.e.

$$\exists csl \in CSL : VP_t(vl) = (CSP(csl), 0).$$

Note that the routes VR_t have to cover the distances traveled by each vehicle with the respective vehicle speeds VS_t in each time step. Hereby, the vehicle speed also can be zero such that the route only contains the current road segment. In particular, zero speed is required to park vehicles at charging stations for one time step. Consequently, the time step resolution also determines the time intervals for charging or discharging vehicle batteries. Furthermore, note that we neglect accelerations and decelerations in the model, which might have a considerable effect on energy consumption [23]. Instead, we assume ideal conditions, which we believe to be sufficient for early phase system design evaluation.

2) Energy storage actions: The energy storage actions ESA_t are modeled as a one-tuple (ESB_t), where

- $ESB_t : ESL \rightarrow \mathbb{R}$ represents their current *balances* (i.e. the amount of energy transferred from or to the parent region).

Note that physically one cannot control the positive or negative energy balance directly. Rather, for a pumped storage hydro power plant one might control a valve limiting the downhill water flow and an electric drive causing the uphill

water flow [25]. In fact, the actual control parameters depend on the specific storage type. We believe that considering the energy balance directly represents the smallest common denominator and, hence, most suitable abstraction in terms of its coverage.

C. Transition function

Finally, the transition function T of the optimal control problem is modeled as a deterministic mapping $\mathbb{S} \times \mathbb{A} \to \mathbb{S}$ with transitions $T(S_t, A_t) = S_{t+1}$ and time point $t \in \mathbb{N}$, where

- S_t represents the system *state* at time point t,
- A_t represents the *action* applied to state S_t, and
- S_{t+1} represents the system *state* at time point $t+1$.

Note that we work with a deterministic transition function to reduce the complexity of the system dynamics. Consequently, one can solve the optimal control problem more easily in practice [26]. However, to obtain higher physical accuracy one might need to introduce a non-deterministic or even probabilistic transition function instead. This transition function could encode the uncertainty about the physical process involved, which occurs due to various simplifications made (see Sections II and III).

Having in mind that $S_t = (VS_t, ESS_t, CSS_t, RS_t)$ and $A_t = (VA_t, ESA_t)$ we decompose T into partial transition functions $VTF, ESTF, CSTF, RTF$, where

- $VS_{t+1} = VTF(VS_t, VA_t)$ represents the *vehicle transition function*,
- $ESS_{t+1} = ESTF(ESS_t, ESA_t)$ represents the *energy storage transition function*,
- $CSS_{t+1} = CSTF(VS_{t+1}, VA_t)$ represents the *charging station transition function*, and
- $RS_{t+1} = RTF(CSS_{t+1}, ESS_{t+1})$ represents the *region transition function*.

Subsequently, we describe the transitions functions for vehicles in Section III-C.1, for energy storages in Section III-C.2, for charging stations in Section III-C.3, and for regions in Section III-C.4.

1) Vehicle transition function: We decompose the vehicle transition function VTF into two partial transition functions $VPTF, VSOCTF$, where

- $VP_{t+1} = VPTF(VP_t, VR_t, VS_t)$ represents the *vehicle position transition function* mapping the current position, route, and speed to the next position and
- $VSOC_{t+1} = VSOCTF(VSOC_t, VP_t, VR_t, VS_t, VB_t)$ represents the *vehicle state of charge transition function* mapping the current state of charge, position, route, speed, and balance to the next state of charge.

Note that the position transition function requires the road segment distances RSD (see Section II-A.2.a) to compute the follow-up vehicle positions on their routes. Furthermore, the vehicle state of charge transition function either requires the driving information (i.e. the position, route, and speed) or the charging balance information (i.e. the energy flow through the charging station) to compute the follow-up state of charge. For future work, we plan on using neural networks for energy consumption estimation for increased accuracy [30].

2) Energy storage transition function: In contrast, we decompose the energy storage transition function $ESTF$ into one partial transition function $ESSTF$, where

- $ESS_{t+1} = ESSTF(ESS_t, ESB_t)$ represents the *energy storage state of charge transition function* mapping the current state of charge and balance to the next state of charge such that $\forall esl \in ESL$ with $ESB_t(esl) < 0$:

$$ESS_{t+1}(esl) = ESS_t(esl) - (1 + \frac{ESE(esl)}{2}) * ESB_t(esl)$$

and for $\forall esl \in ESL$ with $ESB_t(esl) \geq 0$:

$$ESS_{t+1}(esl) = ESS_t(esl) - (1 - \frac{ESE(esl)}{2}) * ESB_t(esl).$$

Note that we use the energy storage efficiency ESE (see Section II-B.2.b) to compute the state of charge during charging. Hereby, the efficiency factor models the energy loss during energy conversion (e.g. electric to potential energy). In particular, the factors models loss in both directions and applies during charging as well as discharging accordingly.

3) Charging station transition function: Then, we decompose the charging station transition function $CSTF$ into one partial transition function $CSBTF$, where

- $CSB_{t+1} = CSBTF(VP_{t+1}, VB_t)$ represents the *charging station balance transition function* mapping the vehicle road segment positions and balances to the charging station balances such that $\forall csl \in CSL$ with $\exists vl \in VL : VP_{t+1}(vl) = (csl, 0)$:

$$CSB_{t+1}(csl) = VB_t(vl).$$

Consequently, the charging station balance equals the vehicle balance.

4) Region transition function: Finally, we decompose the region transition function RTF into three partial transition functions $RETF^{<}, RETF^{>}, RBTF$, where

- $RE^{\sim}_{t+1} = RETF^{\sim}(ESB_{t+1}, CSB_{t+1})$ with $\sim \in \{<, >\}$ represent the *region energy transition functions* aggregating the associated static load profiles, energy storage balances, charging station balances, and subregion balances such that $\forall rl \in RL$:

$$\begin{aligned} RE^{\sim}_{t+1} = & \sum_{sll \in SLL : SLR(sll) = rl} F_{\sim}(SLP(sll)(t+1)) + \\ & \sum_{esl \in ESL : ESR(esl) = rl} F_{\sim}(ESB_{t+1}(esl)) + \\ & \sum_{csl \in CSL : CSR(csl) = rl} F_{\sim}(CSB_{t+1}(csl)) + \\ & \sum_{rl' \in RL : RP(rl') = rl} F_{\sim}(RB_{t+1}(rl')), \text{ where} \end{aligned}$$

the function $F_{\sim} : \mathbb{R} \to \mathbb{R}$ with $\sim \in \{<, >\}$ filters the production and consumption values such that

$$F_{\sim}(x) = \begin{cases} x & \text{if } x \sim 0 \\ 0 & \text{otherwise} \end{cases}, \text{ and}$$

- $RB_{t+1} = RBTF(ESB_{t+1}, CSB_{t+1})$ represents the *region balance transition function* calculating the final balance from the aggregate production and consumption values such that $\forall rl \in RL$:

$$RB_{t+1}(rl) = \begin{cases} RB'_{t+1}(rl) & \text{if } RB'_{t+1}(rl) > 0 \\ RB'_{t+1}(rl) * (1 + RE(rl)) & \text{otherwise} \end{cases}$$

where the balance indicator $RB'_{t+1}(rl)$ is then

$$RB'_{t+1}(rl) = RE^{>}_{t+1}(rl) * (1 + RE(rl)) + RE^{<}_{t+1}(rl).$$

Note that the partial transition functions are defined recursively. Consequently, first the productions, consumptions, and balances have to be computed for the lowest-level regions (i.e. the regions without subregions). Then, the upper levels can be derived one after the other. Furthermore, note that the balance transition function multiplies the production and consumption values with the region efficiency factor RE. In particular, to account for losses over the power lines, the balance indicator RB' first accounts for the production including losses and the consumption. Then, the final balance RB accounts for the remaining consumption including losses. Hereby, the efficiency RE typically ranges in the area of a few percent only and the factor is lower for higher voltage levels.

IV. Requirements on TransP-0 dynamics

While the previous section outlined the state space of TransP-0 system designs, a specific control strategy has not been proposed. In fact, in this paper we do not want to prescribe any specific control strategy. Rather, we want to highlight requirements that control strategies must satisfy in general. Note that additional requirements might be added by transportation and power engineers while exploring the design space. We assume that such requirements are expressed in terms of constraints and objectives of the optimal control problem introduced in Section III. Subsequently, we first discuss the constraints in Section IV-A before elaborating on potential objectives in Section IV-B. Note that constraints and objectives could be defined over the static design space parameters (see Section II) as well. Examples include maximizing the average mechanical and electrical vehicle efficiency or constraining the number of road segments per area unit. However, we did not focus on static requirements in our work yet.

A. Constraints

We provide two basic constraints, which should be part of any reasonable system design. The first constraint ensures that the road segment capacities RSC (i.e. the number of lanes) of the transportation infrastructure TI are not exceeded (see Section IV-A.1). The second constraint ensures that the region capacities RC of the energy infrastructure EI are not exceeded (see Section IV-A.2).

1) Segment capacities: The road segment capacity constraint essentially ensures that no collisions occur in the states $S_t = (VS_t, ESS_t, CSS_t, RS_t)$ with vehicle state $VS_t = (VP_t, VSOC_t)$ of the system dynamics. To derive the constraint, we first define the *overlapping vehicle pair* mapping $OVP_t : RSL \to VL \times VL$, which calculates for each road segment the pairs of overlapping vehicles such that $\forall rsl \in RSL$:

$$OVP_t(rsl) = \{(vl_1, vl_2) \in VL \times VL \mid \exists d_1, d_2 \in \mathbb{R}^+_0 : VP_t(vl_1) = (rsl, d_1) \wedge VP_t(vl_2) = (rsl, d_2) \wedge (|d_1 - d_2| < \frac{(VSE(vl_1) + VSE(vl_2))}{2})\}.$$

The definition expresses that vehicles must reside on the same road segment rsl and their half-sizes $VSE(vl_{1/2})/2$ must be larger than their center distances $|d_1 - d_2|$. Then, we can calculate the *overlapping vehicle set* mapping $OVS_t : RSL \times VL \to \mathcal{P}(VL)$ with power set $\mathcal{P}(\cdot)$, which calculates for each road segment and vehicle the overlapping vehicle pairs such that $\forall rsl \in RSL, vl \in VL$:

$$OVS_t(rsl, vl) = \{vl' \in VL \mid (vl, vl') \in OVP_t(rsl)\}$$

Note that the overlapping vehicle pairs are ordered such that duplicates are avoided by the previous definition. Finally, we can derive the *collision property* mapping $CP_t : RSL \to \mathbb{B}$ with boolean set $\mathbb{B} = \{true, false\}$, which calculates for each road segment whether a collision occurred in state S_t or not such that $\forall rsl \in RSL$:

$$CP_t(rsl) \Leftrightarrow \exists vl \in VL : |OVS_t(rsl, vl)| > RSC(rsl).$$

Consequently, a state is collision-free if for all road segments the collision property is $false$. Note that our constraint definition operates on state information only. However, collisions might occur in between two states, e.g. when one vehicle is overtaking another vehicle on a single-lane road segment within one time step. An advanced constraint definition is required to capture these cases also, but might be more difficult to compute. Alternatively, one might reduce the time step resolution such that these cases do not occur.

2) Region capacities: In contrast, the region capacity constraint ensures that the energy flow through each region does not exceed its capacity limit. Hereby, we have to consider the production and the consumption values separately. In the first case, we require that the aggregate production does not exceed region capacity, i.e. $\forall rl \in RL$:

$$RE^{>}_t(rl) \leq RC(rl)$$

In the second case, we require that the aggregate consumption including the losses over power lines does not exceed region capacity, i.e. $\forall rl \in RL$:

$$-RE^{<}_t(rl) * (1 + RE(rl)) \leq RC(rl)$$

We consider losses for consumption because additional energy has to be transported through the region to cover the demand. In contrast, for the production values no additional energy has to be transported through the region, rather energy is lost while transporting it.

B. Objectives

In addition to constraints (see Section IV-A), our approach supports arbitrary objectives over dynamic properties of the transportation subsystem (see Section II-A) and the energy subsystem (see Section II-B). We do not want to prescribe any particular objectives, but believe it is the designers task to formulate objectives and explore their effect on system structure and dynamics. Among potential objectives of the system dynamics we consider minimizing traveling times, minimizing energy consumption during driving, and operating the energy subsystem infrastructure regions far from their capacity limits. Objectives concerning static properties might include minimizing the number of road segments, minimizing the average slope of the road segments, or maximizing the number of energy subsystem infrastructure regions.

V. Discussion and Outlook

In this paper, we presented the TRANSP-0 design framework for rapidly formulating and evaluating integrated transportation and power system design options. We described the framework in terms of static design parameters, the dynamic aspects of system design and the requirements optimal control strategies have to satisfy. Future work includes increasing the validity of the model, adapting our model to multimodal passenger transportation and logistics problems and establishing further constraints and objectives. Furthermore, we currently work on establishing software tool support.

References

[1] J. Lopes, F. J. Soares, and P. R. Almeida, "Identifying management procedures to deal with connection of electric vehicles in the grid," in *Powertech, 2009 IEEE bucharest*. IEEE, 2009, pp. 1–8.

[2] K. Heussen, S. Koch, A. Ulbig, and G. Andersson, "Unified system-level modeling of intermittent renewable energy sources and energy storage for power system operation," *Systems Journal, IEEE*, vol. 6, no. 1, pp. 140–151, 2012.

[3] D. Dallinger and M. Wietschel, "Grid integration of intermittent renewable energy sources using price-responsive plug-in electric vehicles," *Renewable and Sustainable Energy Reviews*, vol. 16, no. 5, pp. 3370–3382, 2012.

[4] D. F. Allan and A. M. Farid, "A benchmark analysis of open source transportation-electrification simulation tools," in *Intelligent Transportation Systems (ITSC), 2015 IEEE 18th International Conference on*. IEEE, 2015, pp. 1202–1208.

[5] H. Lund and W. Kempton, "Integration of renewable energy into the transport and electricity sectors through v2g," *Energy policy*, vol. 36, no. 9, pp. 3578–3587, 2008.

[6] H. Lund and E. Münster, "Integrated transportation and energy sector co 2 emission control strategies," *Transport Policy*, vol. 13, no. 5, pp. 426–433, 2006.

[7] D. B. Richardson, "Electric vehicles and the electric grid: A review of modeling approaches, impacts, and renewable energy integration," *Renewable and Sustainable Energy Reviews*, vol. 19, pp. 247–254, 2013.

[8] R. Faria, P. Moura, J. Delgado, and A. T. de Almeida, "A sustainability assessment of electric vehicles as a personal mobility system," *Energy Conversion and Management*, vol. 61, pp. 19–30, 2012.

[9] F. Mwasilu, J. J. Justo, E.-K. Kim, T. D. Do, and J.-W. Jung, "Electric vehicles and smart grid interaction: A review on vehicle to grid and renewable energy sources integration," *Renewable and Sustainable Energy Reviews*, vol. 34, pp. 501–516, 2014.

[10] M. Yilmaz and P. T. Krein, "Review of the impact of vehicle-to-grid technologies on distribution systems and utility interfaces," *Power Electronics, IEEE Transactions on*, vol. 28, no. 12, pp. 5673–5689, 2013.

[11] Z. Yang, K. Li, and A. Foley, "Computational scheduling methods for integrating plug-in electric vehicles with power systems: A review," *Renewable and Sustainable Energy Reviews*, vol. 51, pp. 396–416, 2015.

[12] A. Andreotti, G. Carpinelli, F. Mottola, and D. Proto, "A review of single-objective optimization models for plug-in vehicles operation in smart grids part ii: Numerical applications to vehicles fleets," in *Power and Energy Society General Meeting, 2012 IEEE*. IEEE, 2012, pp. 1–8.

[13] Y. Ota, H. Taniguchi, T. Nakajima, K. M. Liyanage, J. Baba, and A. Yokoyama, "Autonomous distributed v2g (vehicle-to-grid) satisfying scheduled charging," *Smart Grid, IEEE Transactions on*, vol. 3, no. 1, pp. 559–564, 2012.

[14] Á. Felipe, M. T. Ortuño, G. Righini, and G. Tirado, "A heuristic approach for the green vehicle routing problem with multiple technologies and partial recharges," *Transportation Research Part E: Logistics and Transportation Review*, vol. 71, pp. 111–128, 2014.

[15] J. Barco, A. Guerra, L. Muñoz, and N. Quijano, "Optimal routing and scheduling of charge for electric vehicles: Case study," *arXiv preprint arXiv:1310.0145*, 2013.

[16] M. D. Galus, R. A. Waraich, F. Noembrini, K. Steurs, G. Georges, K. Boulouchos, K. W. Axhausen, and G. Andersson, "Integrating power systems, transport systems and vehicle technology for electric mobility impact assessment and efficient control," *Smart Grid, IEEE Transactions on*, vol. 3, no. 2, pp. 934–949, 2012.

[17] R. Al Junaibi and A. M. Farid, "A method for the technical feasibility assessment of electrical vehicle penetration," in *Systems Conference (SysCon), 2013 IEEE International*. IEEE, 2013, pp. 606–611.

[18] B. V. Mathiesen, H. Lund, and P. Nørgaard, "Integrated transport and renewable energy systems," *Utilities Policy*, vol. 16, no. 2, pp. 107–116, 2008.

[19] G. Hackenberg, M. Irlbeck, V. Koutsoumpas, and D. Bytschkow, "Applying formal software engineering techniques to smart grids," in *Proceedings of the First International Workshop on Software Engineering Challenges for the Smart Grid*, ser. SE4SG '12. Piscataway, NJ, USA: IEEE Press, 2012, pp. 50–56.

[20] D. Ascher and G. Hackenberg, "Early estimation of multi-objective traffic flow," in *Proceedings of the 3rd International Conference on Connected Vehicles & Expo (ICCVE '14)*. IEEE, 2014, pp. 1056–1057.

[21] ——, "Integrated transportation and power system modeling," in *2015 International Conference on Connected Vehicles and Expo (ICCVE)*. IEEE, 2015, pp. 379–384.

[22] W. Burghout, "Mesoscopic simulation models for short-term prediction," *PREDIKT project report CTR2005*, vol. 3, 2005.

[23] D. W. Gao, C. Mi, and A. Emadi, "Modeling and simulation of electric and hybrid vehicles," *Proceedings of the IEEE*, vol. 95, no. 4, pp. 729–745, 2007.

[24] H. W. Dommel and W. F. Tinney, "Optimal power flow solutions," *IEEE Transactions on Power Apparatus and Systems*, vol. PAS-87, no. 10, pp. 1866–1876, Oct 1968.

[25] E. D. Castronuovo and J. A. P. Lopes, "On the optimization of the daily operation of a wind-hydro power plant," *IEEE Transactions on Power Systems*, vol. 19, no. 3, pp. 1599–1606, Aug 2004.

[26] D. P. Bertsekas, *Dynamic programming and optimal control*. Athena Scientific Belmont, MA, 1995, vol. 1, no. 2.

[27] H. Imine, Y. Delanne, and N. M'sirdi, "Road profile input estimation in vehicle dynamics simulation," *Vehicle System Dynamics*, vol. 44, no. 4, pp. 285–303, 2006.

[28] J. Garcia-Gonzalez, R. M. R. de la Muela, L. M. Santos, and A. M. Gonzalez, "Stochastic joint optimization of wind generation and pumped-storage units in an electricity market," *IEEE Transactions on Power Systems*, vol. 23, no. 2, pp. 460–468, May 2008.

[29] M. Anghel, K. A. Werley, and A. E. Motter, "Stochastic model for power grid dynamics," in *System Sciences, 2007. HICSS 2007. 40th Annual Hawaii International Conference on*. IEEE, 2007, pp. 113–113.

[30] J. Felipe, J. C. Amarillo, J. E. Naranjo, F. Serradilla, and A. Diaz, "Energy consumption estimation in electric vehicles considering driving style," in *Intelligent Transportation Systems (ITSC), 2015 IEEE 18th International Conference on*. IEEE, 2015, pp. 101–106.